Global Journal of Pure and Applied Mathematics.
ISSN 0973-1768 Volume 12, Number 3 (2016), pp. 1979–1999
© Research India Publications
http://www.ripublication.com/gjpam.htm

Elastic and Seismic Model for the Generation of Tsunamis via Lattice Boltzmann Method

Sara Zergani, Z.A. Aziz and K.K. Viswanathan[1]

UTM Centre for Industrial and Applied Mathematics, Ibnu Sina Institute for Scientific and Industrial Research, Universiti Teknologi Malaysia, 81310 Johor Bahru, Johor, Malaysia
Department of Mathematical Sciences, Faculty of Science, Universiti Teknologi Malaysia, 81310 Johor Bahru, Johor, Malaysia

Abstract

An efficient implementation of the Lattice Boltzmann method (LBM) for the numerical simulation of the generation tsunamis, based on Elastic wave equation and P-wave equation is presented. It is provided two examples where the scheme is used to model mechanisms for the generation of seismic waves. Numerical results show good agreement with the theory.

AMS subject classification: 34B60, 35Q20, 65D99.
Keywords: Tsunami, Boltzmann method, Elastic wave, P wave.

1. Introduction

Researchers Thomsen [1] and Steward et al. [2, 3] argue that the earth is probably the tiniest viscoelastic medium that generates attenuation and dispersion effects as a result of absorption losses. Simplistically, the earth is an elastic medium. The researchers further argue that the equation explains the proliferation of seismic waves in the earth is the elastic wave equation, when absorption is ignored. In contrast, the acoustic wave

[1]Corresponding author: E-mail: visu20@yahoo.com, viswanathan@utm.my

equation explains the proliferation of waves in a fluid medium, for instance the ocean. However, the elastic wave equation is written based on the tensor operators acting on vector quantities, while the acoustic wave equation is framed based on the scalar operators acting on scalar quantities. For inverse algorithms to be constructed scalar wave equation is mostly utilized for its simple analysis process and stress-free manipulation functions. In most situations within the elastic earth, it is also argued to be a good approximation, for the behaviour of compressional waves. In view of this fact, the use of the scalar acoustic wave equation has become the primary focus of exploration seismology, for the development of processing and imaging algorithms. However, the situation in global seismology is different, as elastic theory is mostly required from the inception. Perhaps this is as a result of the comparative significance of shear waves used in global seismology. According to researchers Thomson [1] and Steward et al. [2, 3], they argue that interests are currently growing within exploration seismology in the area of enhanced reservoir classification as drawn from the analysis of shear wave and anisotropic behavior. They added that the possibility of the result is that of the recording of elastic wave field using multicomponent data. Consequently, the consideration of elastic wave equation formulation for the processing and imaging algorithms in exploration seismology has become appropriate. Conceivably, it is most evident when dealing with shear waves as well as converted waves. It is also factual that an appropriate treatment for anisotropy basically requires an elastic perspective, no matter whether it is only P-waves or quasi-P waves that are considered. Aki and Richards [4] argue that the elastic wave proliferation theory has been systematically examined using various standard geophysical scripts. According to Auld [5], they argue that various texts have exhaustively explained the theory of anisotropic wave.

2. Formulation of the Problem

2.1. Elastic Wave Generation for Earthquake

The elastic wave equation has been extensively utilized in the explanation of wave generation and proliferation in an elastic medium; examples are seismic waves in the Earth and ultrasonic waves in the human body. Seismic waves are described as the waves of energy which travels through the earth, resulting from an explosion, earthquake, or a volcano. In geophysics, the study of seismic wave proliferation in Earth media is imperative, because it is perceived to be an effective process of assisting people in studying Earth's internal structure. In seismic wave fields modelling, the method of wave equation numerical simulation has played significant role. The underpinning study for seismic wave proliferation is provided by the wave equation simulation which involves the seismic wave dynamics. However, the wave equations in describing the seismic wave fields, employs acoustic wave equations or elastic wave equations. In exploration seismology, the application of acoustic wave equations in the research of seismic wave has recorded progressive improvement. The Earth is considered an inhomogeneous media; as such, an evaluation of the elasticity of the Earth media as well as the vector properties of

seismic waves utilized in theoretical seismology is imperative. Consequently, the accuracy and rationality of basic acoustic approximation is questionable. The use of elastic wave approximation which is more complex and practically reliable in the research of seismic wave is appropriate. Acoustic approximation in essence, could be viewed to be an exceptional situation as well as the explanation to the elastic wave approximation. Hence, acoustic approximation inclines to using elastic wave equations in the description of seismic waves.

2.2. Elastic Wave Equation

The equation of motion for Isotropic solid is

$$\mu\nabla^2 u + (\lambda + \mu)\nabla(\nabla \cdot u) + \rho f = \rho \frac{\partial^2 u}{\partial t^2} \tag{2.1}$$

using the divergence operator identity

$$\nabla^2 u = \nabla(\nabla \cdot u) - \nabla \times (\nabla \times u). \tag{2.2}$$

Equation (2.1) yields as

$$\frac{(\lambda + 2\mu)}{\rho}\nabla(\nabla \cdot u) - \frac{\mu}{\rho}\nabla \times (\nabla \times u) + f = \frac{\partial^2 u}{\partial t^2}. \tag{2.3}$$

The elastic wave equation (2.3) can be written as

$$\alpha^2\nabla(\nabla \cdot u) - \beta^2\nabla \times (\nabla \times u) + f = \frac{\partial^2 u}{\partial t^2} \tag{2.4}$$

where

$$\alpha = \sqrt{\frac{(\lambda + 2\mu)}{\rho}}, \quad \beta = \sqrt{\frac{\mu}{\rho}}, \tag{2.5}$$

α and β are the velocity of the dilatational and shear waves. Equation (2.4) can be further deduced to P and S waves equations.

2.3. P Wave Equation

Multiplying elastic wave equation (2.4) with ∇, the equation reads

$$\alpha^2\nabla \cdot (\nabla(\nabla \cdot u)) - \beta^2\nabla \cdot (\nabla \times (\nabla \times u)) + \nabla \cdot f = \frac{\partial^2}{\partial t^2}(\nabla \cdot u). \tag{2.6}$$

Using the divergence operators

$$\nabla \cdot (\nabla(\nabla \cdot u)) = \nabla^2(\nabla \cdot u), \tag{2.7}$$

$$\nabla \cdot (\nabla \times (\nabla \times u)) = 0. \tag{2.8}$$

Equation (2.6) is reduced to

$$\alpha^2\nabla^2(\nabla \cdot u) + \nabla \cdot f = \frac{\partial^2}{\partial t^2}(\nabla \cdot u). \tag{2.9}$$

Hence P wave equation in scalar form is obtained. It is noted that $\nabla \cdot u$ is a scalar quantity.

2.4. Lattice Boltzmann Method

The Lattice Boltzmann Equation (LBE) can be understood as a discrete Boltzmann Equation. The LBE with a single relaxation time from the BGK model can be expressed as,

$$f_i(x + e_i, t + 1) = f_i(x, t) + \Omega_i(f_i(x, t)), \qquad (i = 0, 1, 2, \ldots, 9) \tag{2.10}$$

where $\Omega_i = \Omega_i(f_i(x, t))$ is a local collision operator.

Carrying out a Taylor expansion in time and space as well as taking the long-wave and low-frequency limit, we obtained the continuum form of the kinetic equation up to the second order for (2.10):

$$\frac{\partial f_i}{\partial t} + e_i \cdot \nabla f_i + \frac{1}{2} e_i \cdot e_i : \nabla\nabla f_i + e_i \cdot \nabla \frac{\partial f_i}{\partial t} + \frac{1}{2}\frac{\partial^2 f_i}{\partial t^2} = \Omega_i. \tag{2.11}$$

where $e_i \cdot e_i : \nabla\nabla f_i$ is the double inner product of two dyads. As such the following multi-scaling expansion is adopted by Frisch, Hasslacher and Pomeau [6]. The time and space derivative is expanded as:

$$\frac{\partial}{\partial t} = \varepsilon \frac{\partial}{\partial t_1} + \varepsilon^2 \frac{\partial}{\partial t_2}, \quad \frac{\partial}{\partial x} = \varepsilon \frac{\partial}{\partial x_1} \tag{2.12}$$

where ε is the expansion parameter as explained in the previous section. The above formula indicates that the diffusion time scale, t_2, is much slower than the convection time scale t_1. Similarly, the one-particle distribution, f_i is expanded about the local equilibrium distribution,

$$f_i = f_i^{eq} + \varepsilon f_i^{(1)} + \varepsilon^2 f_i^{(2)}. \tag{2.13}$$

Inserting f into the collision operator, we have,

$$\Omega_i(f) = \Omega_i(f_i^{eq} + \varepsilon \frac{\partial \Omega_i(f_i^{eq})}{\partial f_j} \partial f_j^{(1)} + O(\varepsilon^2). \tag{2.14}$$

The Chapman-Enskog theory requires $\Omega_i(f_i^{eq}) = 0$. Neglecting second and higher order terms, we have the linearized form of the collision operator $\Omega_i(f) = \varepsilon M_{ij} f_j^{(1)}$ where $M_{ij} = \dfrac{\partial \Omega_i(f_i^{eq})}{\partial f_j}$.

If we further assume that the local particle distribution relaxes to an equilibrium state at a single rate $\dfrac{\partial \Omega_i}{\partial f_j} = -\dfrac{1}{\tau}\delta_{ij}$ with a universal time scale τ (the 7 BGK form [7]), we arrive at the following linearized form:

$$\Omega_i = -\frac{1}{\tau}(f_i - f_i^{eq}). \tag{2.15}$$

It is observed that both the $\sum_i \Omega_i = 0$ and $\sum_i e_i \Omega_i = 0$. The parameter τ is interpretable to mean the relaxation time clue to collisions. The function f_i^{eq} is the enforced equilibrium distribution for this Boltzmann system. It may be shown from equations (2.10) and (2.15) that f_i asymptotically approaches the enforced distribution f_i^{eq}, if the latter is positive everywhere and τ is greater than $\frac{1}{2}$ as mentioned by Luo [8]. In order for the fluid to have Galilean-invariant convection and a pressure which does not depend on velocity, the equilibrium distribution f_i^{eq} is assumed to be,

$$f_i^{eq} = \frac{\rho}{m}\left(\frac{1-\alpha}{6} + \frac{1}{3}e_i \cdot v + \frac{2}{3}(e_i)_\alpha (e_i)_\beta v_\alpha v_\beta - \frac{1}{6}v^2\right), \quad f_0^{eq} = \frac{\rho}{m}(\alpha - v^2) \tag{2.16}$$

where α is a free parameter related to the sound speed as shown below. From (2.11), we can obtain the following equations,

$$\frac{\partial f_i^{eq}}{\partial t_1} + e_i \nabla_1 f_i^{eq} = -\frac{\partial f_i^1}{\tau} \tag{2.17}$$

$$\frac{\partial f_i^{(1)}}{\partial t_2} + \left(1 - \frac{1}{2\tau}\right)\left(\frac{\partial f_i^{(1)}}{\partial t_1} + e_i \cdot \nabla_1 f_i^{(1)}\right) = -\frac{\partial f_i^2}{\tau}. \tag{2.18}$$

The momentum equation can be written as:

$$\frac{\partial nv}{\partial t} + \nabla \cdot \Pi = 0 \tag{2.19}$$

where the momentum flux density tensor Π is in the form

$$\Pi_{\alpha\beta} = \sum_i (e_i)_\alpha (e_i)_\beta \left[f_i^{eq} + \left(1 - \frac{1}{2\tau}\right) f_i^{(1)}\right] \tag{2.20}$$

where $(e_i)_\alpha$ is the a component of the velocity vector e_i. Inserting equation (2.16) into Π and using the first equation in (2.18), one obtains, to zero order in the small parameter of the Chapman-Enskog expansion.

$$\Pi_{\alpha\beta}^{(0)} = \sum_i (e_i)_\alpha (e_i)_\beta f_i^{eq} = 3n\frac{1-\alpha}{6}\delta_{\alpha\beta} + nv_\alpha v_\beta \tag{2.21}$$

$$\Pi_{\alpha\beta}^{(1)} = -\tau\left\{\frac{\partial}{\partial t}\Pi_{\alpha\beta}^{(0)} + \frac{\partial}{\partial x}\sum_i (e_i)_\alpha (e_i)_\beta (e_i)_\gamma f_i^0\right\} \tag{2.22}$$

to first order. The final form of the macroscopic equations becomes,

$$\frac{\partial \rho}{\partial t} + \frac{\partial(\rho v_\beta)}{\partial x_\beta} = 0,$$
$$\rho \frac{\partial v_\alpha}{\partial t} + \rho v_\beta \frac{\partial(v_\alpha)}{\partial x_\beta} = -\frac{\partial \rho}{\partial x_\alpha} + \frac{\partial}{\partial x_\beta}\left[\frac{\lambda}{\rho}\left(\frac{\partial(\rho v_\gamma)}{\partial x_\gamma} + v_\alpha \frac{\partial \rho}{\partial x_\beta} + v_\beta \frac{\partial \rho}{\partial x_\alpha}\right) + \frac{\partial}{\partial x_\beta}\left[\mu\left(\frac{\partial v_\beta}{\partial x_\alpha} + \frac{\partial v_\alpha}{\partial x_\beta}\right)\right]\right] \tag{2.23}$$

and

$$p = \frac{1-\alpha}{2}\rho. \tag{2.24}$$

In the above equations, p is the pressure and the sound speed, c_s is $\sqrt{\frac{1-\alpha}{2}}$. The shear viscosity μ is $\frac{(2\tau-1)}{8}$ and the bulk viscosity, λ is $\frac{\left(\tau-\frac{1}{2}\right)(2\alpha-1)\rho}{4}$. The above formula converges to the actual incompressible Navier-Stokes equations only when the types of the solidity in the second viscosity phrase on the right side part of the formula are little. Since the gradients of the solidity are $O(u^2)$ [9], the unphysical conditions in equation (2.22) are $O(u^3)$. Thus, although the science contains compressibility results, one may come randomly near to fixing incompressible Series by decreasing the Mach variety $M = \frac{v}{c_s}$. To fix incompressible liquid moves by conventional mathematical techniques, such as limited distinction or finite-element, one must cope with a Poisson formula for the stress phrase that is caused by the procession situation and the strength formula. Here we can see that the remedy of the Navier-Stokes formula can be acquired through the lattice-Boltzmann formula in (2.10) and the stress results on the strength formula are managed by a formula of condition. Solution of the Poisson formula is actually prevented by soothing the incompressibility needed. It may be suggested that CA (Cellular Automaton) techniques are most carefully relevant to pseudo-compressible methods [10, 11] for fixing incompressible liquid moves. There may still be some variations between the incompressible Navier-Stokes formula and the macroscopic actions of the discrete-velocity Boltzmann equations because of the asymptotic characteristics of the Chapman-Enskog technique. These variations could be linked to greater purchase conditions, such as the Burnett conditions, or as little diversions from the above regards for the kinematic viscosity. However, Burnett conditions are required to become minimal as the international Knudsen variety $K_n = \frac{1}{l}$ becomes little, where l is the mean free direction. Since the Knudsen variety is proportionate to the Mach variety separated by the Reynolds variety, the Burnett conditions may be arranged with other "compressibility" results and should become less as the Mach variety techniques zero for a set Reynolds variety. It should be described that the mathematical execution for (2.10) is uncomplicated.

At every phase, one determines a new f_i' on each lattice: $f_i' = f_i - \dfrac{f_i - f_i^{eq}}{\tau}$ where f_i and f_i^{eq} are all known features. Then, f_i' is adverted to a new place, becoming a new f_i. Using the new f_i, the solidity and speed can be measured again. There are a variety of variations between the lattice-Boltzmann technique and the lattice-gas technique. Without going into the information, the latter strategy includes the following characteristics of contaminants on a lattice. The lattice-gas strategy includes only Boolean features and hence has no mathematical circular off mistakes and instabilities, contrary to the floating-point features in the lattice-Boltzmann technique. The problems are that the particle-collision guidelines must be clearly designed so as to get the preferred stability submission and hydrodynamical qualities. Moreover, appropriate mathematical earnings must be taken to acquire liquid amounts. However, the lattice-Boltzmann technique is just like a precise finite-difference plan, fixing the discretized kinetic formula by a Lagrangian upwind plan [12, 13, 14], which is conditionally constant. Balance and precision studies have been offered lately by [12, 15], respectively. It has been proven from their studies that the lattice-Boltzmann techniques are second purchased, precisely both in efforts and area. To make sure mathematical stability, the pleasure time should not be less than $\dfrac{1}{2}$ [12] for other parameter dependencies of the soundness of lattice-Boltzmann methods.

2.5. Equilibrium Distribution Function Lattice Gas Method (For Fluids)

Sound trend reproduction in a sticky liquid and liquid huge transportation is made using the lattice Bhatnagar-Gross-Krook (BGK) method [16]. The BGK method has been designed from the lattice gas automaton design for the remedy of the Navier-Stokes formula [6] specific information of lattice gas techniques is given by [17, 18]. In the BGK plan a frequent lattice is seeded with solidity submission features $f_i(x, t)$ along each lattice node x in the direction i. The process then includes fixing the Boltzmann formula where e_i is the speed vector along weblink i in a rectangle (Figure 1). The formula records for the return of strength through crashes at the lattice nodes and then reproduction of the post collision submission feature along the lattice hyperlinks. Complicated geometries are involved in the design by basically giving a Boolean varying to each lattice node, showing whether the node is a firm strong or liquid location.

In the BGK lattice method, pseudo fluid particles propagate along the lattice vectors. These pseudo particles collide at the lattice nodes, conserving density and momentum. This method reproduces the Navier-Stokes equation and can be used to model fluid motion and/or acoustic wave propagation.

The equilibrium distribution for a two-dimensional square lattice with nine vectors e_i along each lattice direction including a zero-velocity vector (denoted D2Q9 by [19]) is given by

$$f_i^{eq}(x, t) = \rho(x)[A_a + B_a(e_i \cdot u) + C_a(e_i \cdot u)^2 + D_a u^2], \tag{2.25}$$

with $a = 0$ for $|e_i| = 0$, $a = 1$ for $|e_i| = 1$, and $a = 2$ for $|e_i| = \sqrt{2}$.

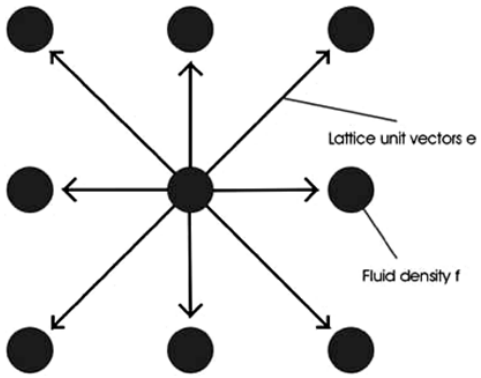

Figure 1: Propagation of pseudo fluid particles propagate along the lattice vectors.

The constants A_a, B_a, C_a and D_a are given by

$$A_0 = d_0,\ A_1 = \frac{(1-d_0)}{5},\ A_2 = \frac{(1-d_0)}{20},\ B_0 = 0,\ B_1 = \frac{1}{3},\ B_2 = \frac{1}{12}$$
$$C_0 = 0,\ C_1 = \frac{1}{2},\ C_2 = \frac{1}{8},\ D_0 = -\frac{2}{3},\ D_1 = -\frac{1}{6},\ D_2 = -\frac{1}{24} \tag{2.26}$$

where d_0 is an arbitrary constant. The macroscopic equations are derived from a Chapman-Enskog expansion that results in the continuity equation and the Navier-Stokes equation for an isothermal, incompressible fluid:

$$\partial_t \rho + \partial_\alpha \rho v_\alpha = 0, \tag{2.27}$$

$$\partial_t \rho v_\alpha + \partial_\alpha \rho v_\alpha v_\gamma = -\partial_\alpha \left[\frac{3}{5}(1-d_0)\right]\rho + v\partial_\gamma \partial_\gamma \rho v_\alpha - \partial_\gamma \xi \partial_\alpha \rho v_\gamma. \tag{2.28}$$

The kinematic viscosity (v) and (ξ) are given by

$$v = \frac{(2\tau - 1)}{6}, \quad \xi = \left(\tau - \frac{1}{2}\right)\left(1 + \frac{9d_0}{15}\right). \tag{2.29}$$

For an ideal gas the pressure is given by $p = c_s^2 \rho$, which gives the speed of sound as $c_s = \sqrt{\frac{3(1-d_0)}{5}}$.

This strategy has been used for the reproduction of straight line and nonlinear audio surf in a sticky liquid using the D2Q7 ingredients [20]. The technique is limited to low Mach figures and to little solidity modifications of only a few percent [20]. Latest techniques have been suggested to design common liquids at great Mach moves by such as more than one distinct speed [21]. These qualities are essential in considering several possible resource systems in a volcanic establishing, such as blocked circulation characteristics as a possible leading to procedure [22, 23, 24]. However, those computationally

more costly techniques are not used here. A critical facet of this plan is that it allows us to design both huge transportation and/or audio trend reproduction in the liquid.

$$f_i^{eq}(x,t) = \begin{cases} \rho[A + B(e_i \cdot u) + C(e_i \cdot u)^2 + Du^2], & i = 1, \ldots, 6 \\ \rho[A_0 + D_0 u^2], & i = 0 \end{cases} \tag{2.30}$$

$$A_0 = d_0,\ A = \frac{(1-d_0)}{6},\ B = \frac{1}{3},\ C = \frac{2}{3},\ D_0 = -1,\ D = -\frac{1}{6} \tag{2.31}$$

where d_0 is an arbitrary constant. This determines the equilibrium distribution function which is applied here. In general, a different equilibrium distribution function can be used if different fluid properties are required.

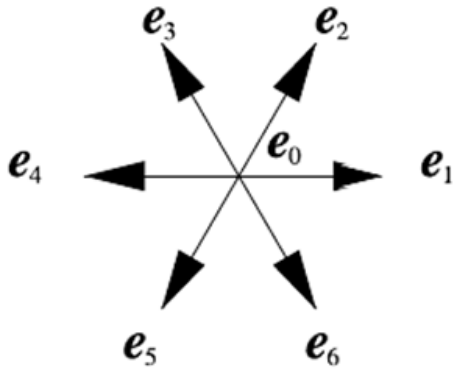

Figure 2: The hexagonal grid on which the simulations are performed, the vectors e_1, e_6 are unit vectors along the directions of the grid and e_0 is the null vector.

The continuity and Navier–Stokes equations for an incompressible, isothermal fluid in two dimensions:

$$\partial_t \rho + \partial_\alpha \rho v_\alpha = 0, \tag{2.32}$$

$$\partial_t \rho v_\alpha + \partial_\alpha \rho v_\alpha v_\beta = -\partial_\alpha \left[\frac{1}{2}(1-d_0)\right]\rho + v\partial_\beta \partial_\beta \rho v_\alpha - \partial_\beta \xi\, \partial_\alpha \rho v_\beta \tag{2.33}$$

where

$$v = \frac{1}{4}\left(\tau - \frac{1}{2}\right), \quad \xi = \left(\tau - \frac{1}{2}\right)\left[\frac{1}{2} - \frac{1}{2}(1-d_0)\right] \tag{2.34}$$

are the kinematic shear and bulk viscosities.

The pressure term in equation (2.33) is $p = \dfrac{\rho}{2}(1-d_0)$ which, for a perfect gas, gives the speed of sound as $c_s = \sqrt{\dfrac{1}{2}(1-d_0)}$.

The lattice Boltzmann technique is of the latter kind, being centred in mesoscopic kinetic concept and used for models of macroscopic behaviour. It can be seen as either

a progress of the mature technique of lattice gas automata, or as a discretisation of the Boltzmann formula, which is a basic of kinetic concept. The technique performs by monitoring the activity and connections of compound withdrawals within the computing sector. Since its start in 1988, the technique has been used for a variety of acoustically relevant reasons, such as models of sound loading, surprise methodologies, compound movement in ultrasound examination areas, circulation models in reed device mouth pieces, and research of glottal circulation.

2.6. Boundary Condition

The plan described above cannot be used at the boundary of the lattice unless unique conditions are created. The issue is that a node at the boundary cannot collect the inbound contaminants from a non-existent neighbour. However, in the actual trend propagations the behaviour at the boundary is determined by its boundary circumstances. Illustrations of some boundary circumstances in seismic modelling are the free surface place and taking in boundary circumstances. The essence of this strategy is to obtain a regards between the inbound contaminants and confident contaminants from the given boundary circumstances. Consider a speed route i from a losing neighbour website into the trend place area. Let f_i^{IN} signify the inbound compound submission along e_i and f_i^{OUT} the confident compound submission along e_i. Now using formula (2.16) the following interaction between f_i^{IN} and $f_i^{\mathrm{OUT}} = \dfrac{\rho}{m}$ is derivable

$$f_i^{\mathrm{IN}} + f_i^{\mathrm{OUT}} = \frac{1-\alpha}{2}\frac{\rho}{m}, \tag{2.35}$$

$$f_i^{\mathrm{IN}} - f_i^{\mathrm{OUT}} = \frac{\rho}{m}\frac{e_i \cdot v}{c^2}. \tag{2.36}$$

The first equation shows immediately how, in general, pressure (or density) boundary conditions can be imposed. A special case of a pressure boundary condition is the free surface where $\Delta P = 0$ (or $\rho = \rho_0$) and

$$f_i^{\mathrm{IN}} = \frac{1-\alpha}{2}\frac{\rho}{m} - f_i^{\mathrm{OUT}}. \tag{2.37}$$

To implement an absorbing boundary condition, for example, the condition B-1 of [25],

$$\frac{\partial(\Delta P)}{\partial t} = c_s \frac{\partial(\Delta P)}{\partial x}. \tag{2.38}$$

Upon substitution into equation (2.23), we obtain an approximation to the particle velocity estimate

$$\rho_0 v(x,t) = \rho_0 v\left(x + e_i \Delta t, t\right) + \frac{c_s}{\rho_0}\left[\rho(x,t) + \rho\left(x + e_i \Delta t, t\right)\right]. \tag{2.39}$$

where ρ and v calculated according conservation laws. Relating this to (2.36), f_i^{IN} is achievable.

3. Results and Discussion

In the following, to test LBM model proposed in the above section, numerical simulations of P- wave equation are performed. There are two types of medium for P wave is given as:

Test 1: A test problem, P wave is non-diffusive given that quantity η_α is real. Figures 3 to 13 are plotted for the non-diffusive P wave with $-5 \leq x \leq 5$, $k = 1$, $\alpha = 2\ m/s$, $c_\alpha = 4\ m/s$.

$$u_p = A\eta_\alpha \exp(-ik\eta_\alpha z) \exp[ik(c_\alpha t - x)] \quad \text{for} \quad c_\alpha > \alpha. \tag{3.1}$$

Test 2: A test problem, P wave is diffusive given that quantity η_α is complex. Figures 14 to 23 are plotted for the diffusive P wave with $\eta_\alpha = i\eta_\alpha$, $-5 \leq x \leq 5, k = 1, \alpha = 4\,m/s$, $c_\alpha = 2\ m/s$.

$$u_p = Ai\eta_\alpha \exp(-k\eta_\alpha z) \exp[ik(c_\alpha t - x)] \quad \text{for} \quad c_\alpha < \alpha. \tag{3.2}$$

When discussing the phenomenon of an earth quake, the primary wave is called P wave. A numerical solution of the P wave is utilized to solve both the diffusive and non-diffusive of the P wave using D2Q9 squared lattice. The numerical computations utilized the 101×101 square lattices, with, $\Delta x = 1500$, $\Delta y = 150$, $\Delta t = 2000$, and $\tau = 1$, the method implored is sensitive to choice of values for the single relaxation time over the range considered. The LBM is a discrete numerical method; it may suffer instability like any other numerical methods, but by using suitable time relaxation values, lattice size and time step, such instabilities could be minimized. The kinematic viscosity v must be positive, $v = \dfrac{(2\tau - 1)}{6} > 0$. Slip boundary condition is used for the side walls. Results are plotted using the inflow and outflow scheme as seen in the figures, a comparison with the analytical solutions with the available numerical methods was done and the error realized is around (1×10^{-4}).

Table 1: Values of various parameters used for non-diffusive and diffusive P wave test-case

Relaxation time τ	1.00
Real channel length rx	$1400m$
dx	$0.05m$
ρ	1.00
u_x	0
u_y	0

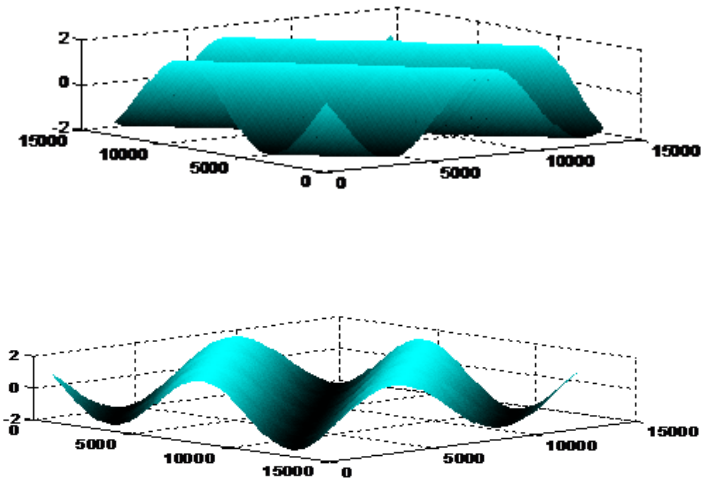

Figure 3: Non-diffusive characteristic of P wave at time $t = 1.00$.

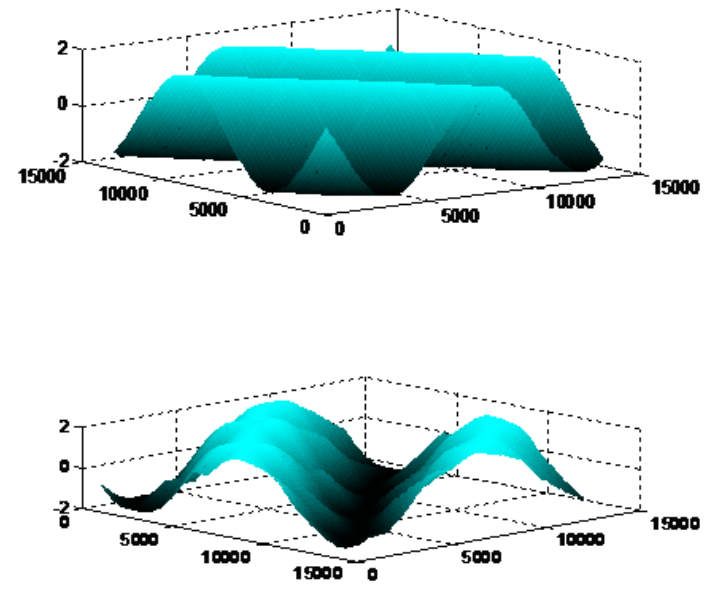

Figure 4: Non-diffusive characteristic of P wave at time $t = 10.00$.

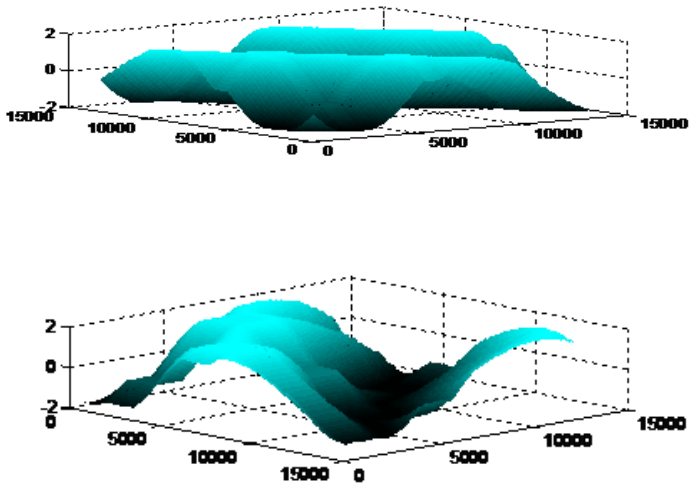

Figure 5: Non-diffusive characteristic of P wave at time $t = 20.00$.

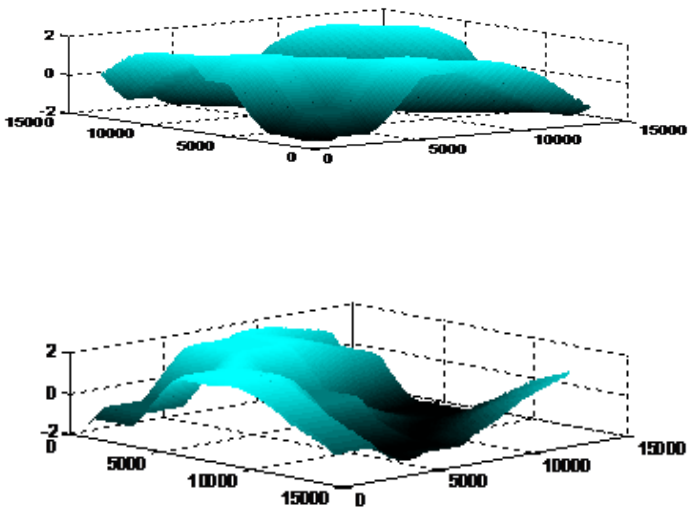

Figure 6: Non-diffusive characteristic of P wave at time $t = 40.00$.

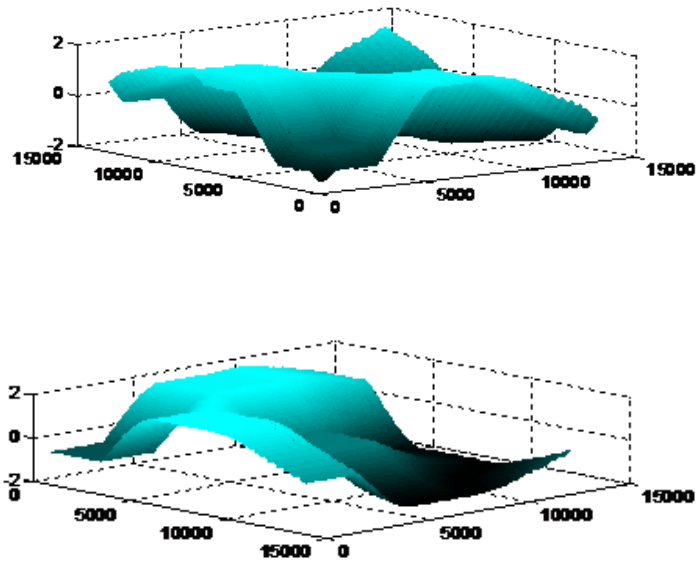

Figure 7: Non-diffusive characteristic of P wave at time $t = 50.00$.

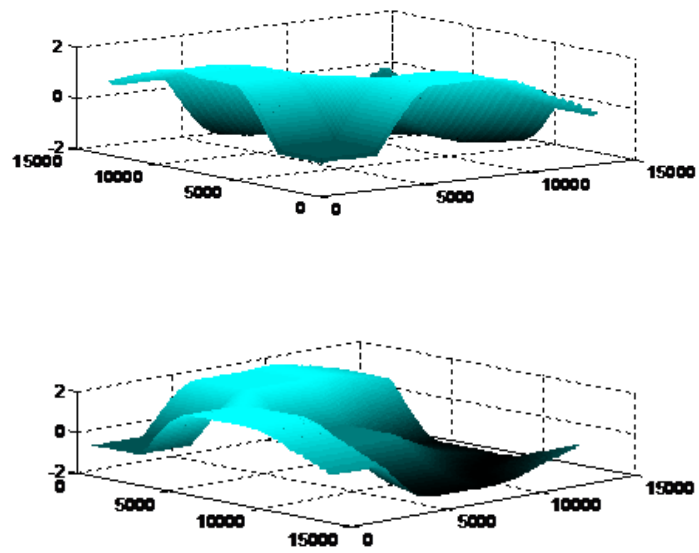

Figure 8: Non-diffusive characteristic of P wave at time $t = 60.00$.

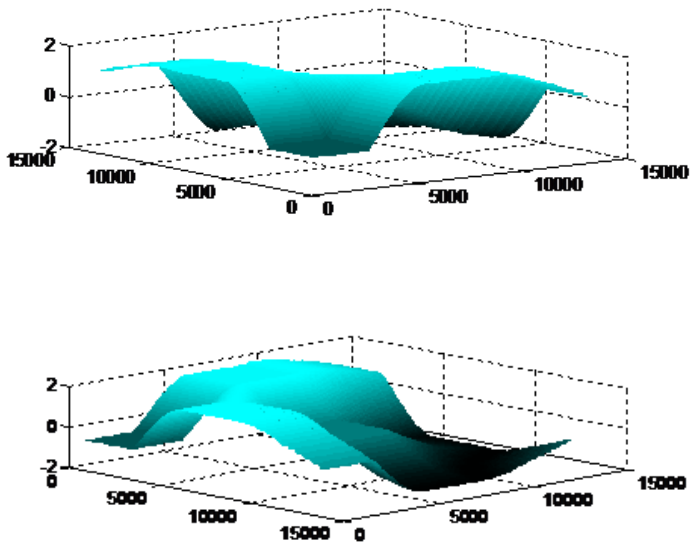

Figure 9: Non-diffusive characteristic of P wave at time $t = 70.00$.

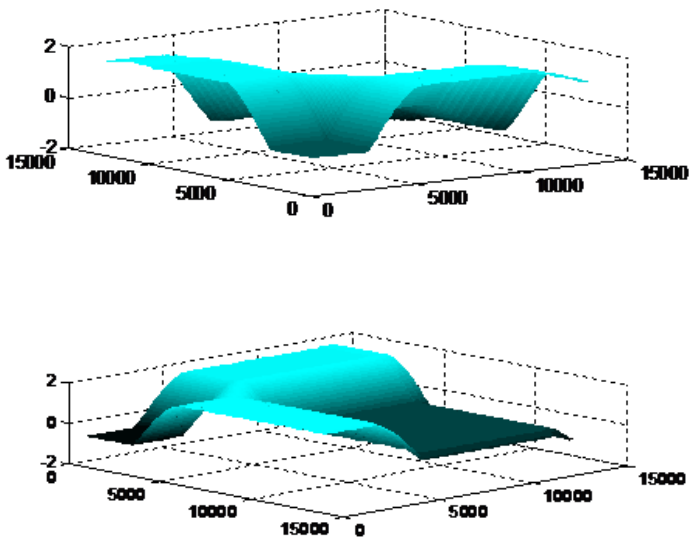

Figure 10: Non-diffusive characteristic of P wave at time $t = 80.00$.

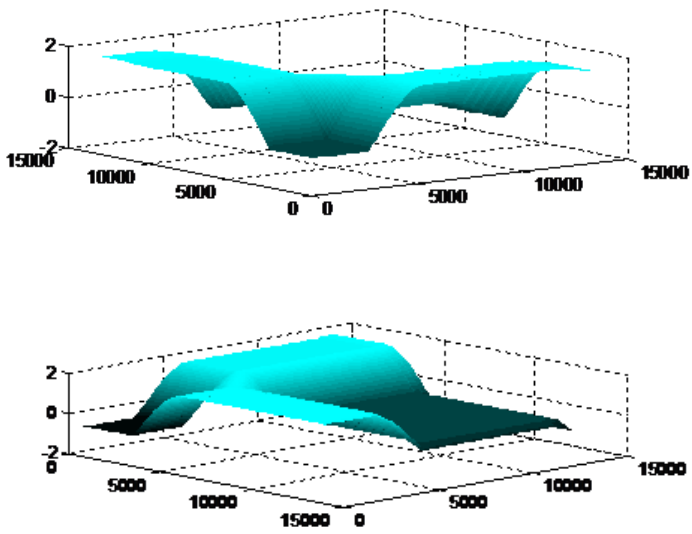

Figure 11: Non-diffusive characteristic of P wave at time $t = 100.00$.

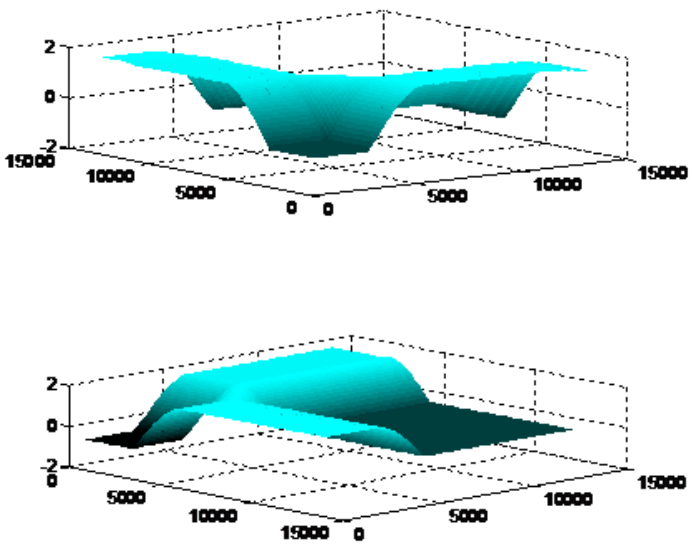

Figure 12: Non-diffusive characteristic of P wave at time $t = 110.00$.

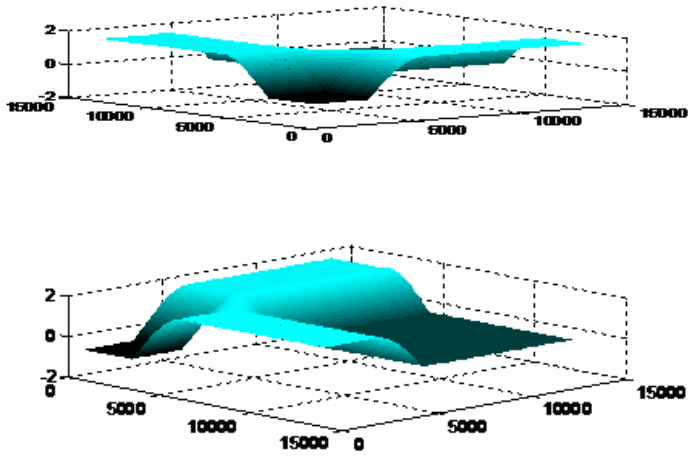

Figure 13: Non-diffusive characteristic of P wave at time $t = 600.00$.

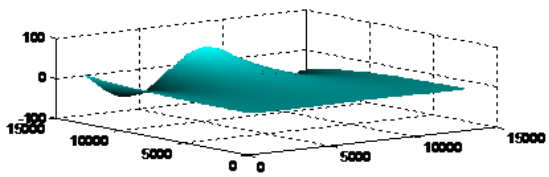

Figure 14: Diffusive characteristic of P wave at time $t = 1.00$.

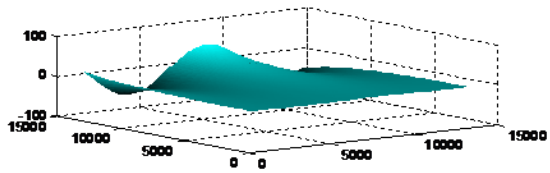

Figure 15: Diffusive characteristic of P wave at time $t = 2.00$.

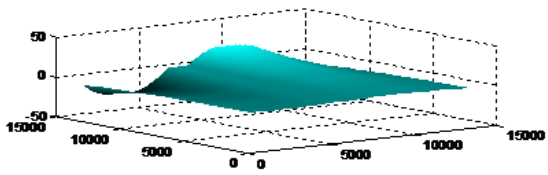

Figure 16: Diffusive characteristic of P wave at time $t = 10.00$.

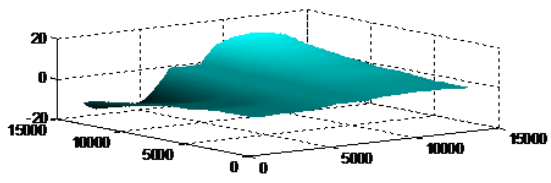

Figure 17: Diffusive characteristic of P wave at time $t = 20.00$.

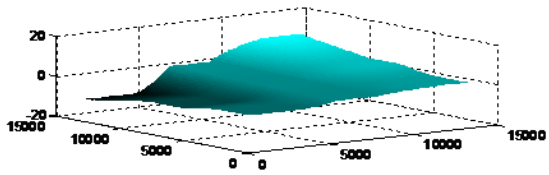

Figure 18: Diffusive characteristic of P wave at time $t = 30.00$.

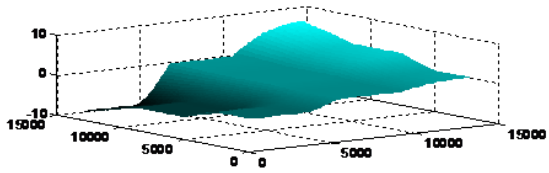

Figure 19: Diffusive characteristic of P wave at time $t = 40.00$.

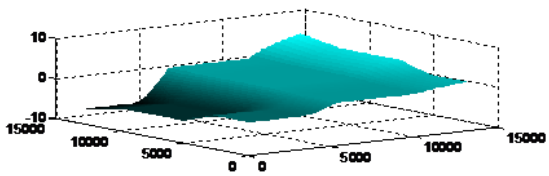

Figure 20: Diffusive characteristic of P wave at time $t = 50.00$.

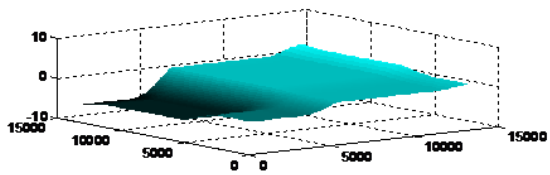

Figure 21: Diffusive characteristic of P wave at time $t = 100.00$.

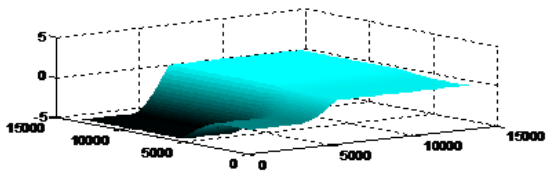

Figure 22: Diffusive characteristic of P wave at time $t = 200.00$.

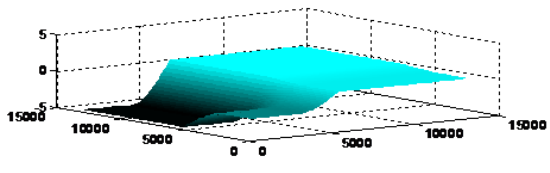

Figure 23: Diffusive characteristic of P wave at time $t = 1000.00$.

4. Conclusion

The use of lattice Boltzmann model for simulating nonlinear generative elastic waves has been considered. It has been seen that a range of problems in nonlinear elastics are within the dynamic range of the lattice Boltzmann model and the application of the technique has been demonstrated. This was done by simulating the development of a P-wave front from an initially nonlinear wave. The results of the simulation agreed well with theory, suggesting that the lattice Boltzmann model is indeed a useful approach to simulating nonlinear elastic phenomena.

It can be found that the LBM results are in excellent agreement with the analytical solution Ching [26] thesis and the numerical results are more comparable and effective with Dutyk [27] thesis .The present model can be used to solve more kinds of problems S-waves and P-waves in elastic wave equation in addition We can apply this method to more complicated systems arising in fluid dynamics.

Acknowledgment

The authors thankfully acknowledge the financial support from Ministry of Higher Education Malaysia, MOHE, GUP Project Vote No. 11H90 and MOHE, FRGS Project Vote No. 4F354 under the Research Management Centre (RMC), Universiti Teknologi Malaysia, Johor Bahru, Johor, Malaysia.

References

[1] Thomsen, L., 1999, "Converted-Wave Reflection Seismology Over Inhomogeneous Anisotropic Media," Geophysics, 64, pp. 678–690.

[2] Stewart, R. R., Gaiser, J. E., Brown, J. R., and Lawton, D. C., 2002, "Converted-Wave Seismic Exploration: Methods," Geophysics, 67, pp. 1348–1363.

[3] Stewart, R. R., Gaiser, J. E., Brown, J. R., and Lawton, D. C., 2003, "Converted-Wave Seismic Exploration: Applications," Geophysics, 68, pp. 40–57.

[4] Aki, K., and Richards, P.G., 2002, Quantitative Seismology, University Science Books, Sausalito, CA.

[5] Auld, B.A., 1990, Acoustic Fields and Waves in Solids, Krieger Publ. Co.

[6] Frisch, U., Hasslacher, B., and Pomeau, Y., 1986, "Lattice-Gas Automata for the Navier-Stokes Equation," Physical Review Letters, 56(14), pp. 1505–1508.

[7] Bhatnagar, P. L., Gross, E. P., and Krook, M., 1954, "A Model for Collision Processes in Gases. I. Small Amplitude Processes in Charged and Neutral One-Component Systems," Phys. Rev., 94, pp. 511–525.

[8] Luo, L., 1997, "Symmetry Breaking of Flow in 2D Symmetric Channels: Simulations by Lattice-Boltzmann Method," Int. J. Modern Phys. C, 8(4), pp. 859–867.

[9] Majda, A., 1984, Compressible Fluid and Systems of Conservation Laws in Several Space Variables, Springer-Verlag, New York.

[10] Messina, J. P., Gilkeson, G. S., and Pisetsky, D. S., 1991, "Stimulation of in Vitro Murine Lymphocyte Proliferation by Bacterial DNA," Journal of Immunology, 147(6), pp. 1759–764.

[11] Ramshaw, I. A., Fordham, S. A., Bernard, C. C.,Maquire, D., Cowden, W. B., and Willenborg, D. O., 1997, "DNA Vaccines for the Treatment of Autoimmune Disease," Immunology and Cell Biology, 75(4), pp. 409–413.

[12] Sterling, J. D., and Chen, S., 1996, "Stability Analysis of Lattice Boltzmann Methods," J. Comp. Phys., 123(1), pp. 196–206.

[13] Skordos, P. A., 1993, "Initial and Boundary Conditions for the Lattice Boltzmann Method," Phys. Rev. E, 48, pp. 4823–4842.

[14] Ancona, M. G., 1994, "Fully-Lagrangian and Lattice-Boltzmann Methods for Solving Systems of Conservation Equations," J. Comp. Phys., 115, pp. 107–20.

[15] Reider, M. B., and Sterling, J. D., 1995, "Accuracy of Discrete-Velocity BGK Models for the Simulation of the Incompressible Navier-Stokes Equations," Computers and Fluids, 24(4), pp. 459–467.

[16] Qian, Y. H., 1993, "Simulating Thermohydrodynamics with Lattice BGK Models," Journal of Scientific Computing, 8, pp. 231–242.

[17] Chen, S., and Doolen, G. D., 1998, "Lattice Boltzmann Methods for Fluid Flows," Annu. Rev. Fluid Mech., 30, pp. 329–364.

[18] Buick, J. M., Greated, C. A., and Campbell, D. M., 1998, "Lattice BGK Simulation of Sound Waves," Europhys. Lett., 43(3), pp. 235–240.

[19] Buick, J. M., Buckley, C. L., Greated, C. A., and Gilbert, J., 2000, "Lattice Boltzmann BGK Simulation of Non-Linear Sound Waves: The Development of a Shock Front," J. Phys. A: Math. Gen., 33, pp. 3917–3928.

[20] Yan, G., and Zhang, J., 2009, "A Higher-Order Moment Method of the Lattice Boltzmann Model for the Korteweg-De Vries Equation," Mathematics and Computers in Simulation, 79(5), pp. 1554–1565.

[21] Morrissey, M. M., and Chouet, B. A., 1997, "A Numerical Investigation of Choked Flow Dynamics and Its Application to the Triggering of Long-Period Events at Redoubt Volcano, Alaska," J. Geophys. Res. B: Solid Earth, 102(B4), pp. 7965–7983.

[22] Chouet, B., 1988, "Resonance of a Fluid-Driven Crack: Radiation Properties and Implications for the Source of Long-Period Events and Harmonic Tremor," J. Geophys. Res. Solid Earth, 93(B5), pp. 4375–4400.

[23] Chouet, B., 2003, "Volcano Seismoloy," Pure Appl. Geophys., 160, pp. 739–788.

[24] del Valle-Garcia, R., and Sa´nchez-Sesma, F. J., 2003, "Rayleigh Waves Modeling using an Elastic Lattice Model," Geophys. Res. Lett., 30(16), pp. 1866, doi:10.1029/2003GL017600.

[25] Clayton, R. W., and Engquist, B., 1980, "Absorbing Boundary Conditions for Wave-Equation Migration," Geophysics, 45(5), pp. 895–904.

[26] Ching, D. L. C., 2011, "Mathematical Modelling of Seismic Wave Propagation," Ph.D. Thesis, Universiti Teknologi Malaysia, Johor, Malaysia.

[27] Dutyk, D., 2008, "Mathematical Modeling of Tsunami Waves," Ph.D. Thesis, Mathematics [math], Ecolenormalesuperieure de Cachan - ENS Cachan, 2007, English.